JOURNAL OF APPLIED ELECTROCHEMISTRY 25 (1995) 940–946

Kinetics and mechanism of the magnesium electrode reaction in molten magnesium chloride

A. KISZA, J. KAŹMIERCZAK

Institute of Chemistry, University of Wrocław, 50383 Wrocław, Poland

B. BØRRESEN, G. M. HAARBERG, R. TUNOLD

Department of Electrochemistry, NTH, University of Trondheim, 7034 Trondheim, Norway

Received 13 June 1994; revised 7 March 1995

Using electrochemical impedance spectroscopy (EIS) and relaxation method with galvanostatic perturbation (RM) the kinetics and mechanism of the magnesium electrode reaction in pure molten $MgCl_2$ have been determined at several temperatures. A three-step electrode process has been found, the high frequency process being pure charge transfer with the low frequency process showing mixed charge transfer–diffusion character. The low frequency step has also been treated as a preceding chemical reaction followed by charge transfer. On the basis of the corresponding exchange current densities and Warburg diffusion impedance, a mechanism of the overall electrode reaction in this melt is proposed.

1. Introduction

Electrochemical studies of the deposition of magnesium from molten salts have mainly been carried out in rather dilute solutions of $MgCl_2$ in mixtures of alkali chlorides. In these cases the rate of the cathode process was found to be controlled by diffusion of the dissolved divalent magnesium species. Literature data on the charge transfer reaction are scarce.

Rao [1] found the deposition of Mg from NaCl–KCl–$CaCl_2$ melts with $MgCl_2$ to be a reversible two-electron process. Tunold [2] studied the cathode reaction in dilute solutions of $MgCl_2$ in molten NaCl–KCl on different substrates. The rate of the magnesium deposition was essentially found to be governed by diffusion, but effects of codeposition of sodium and interaction between magnesium and the substrate were observed. The use of transient techniques, for example, voltammetry at high scan rates and potential step measurements at short times, revealed some irreversibility of the discharge at 750 °C, corresponding to an exchange current density of about 2 A cm^{-2}.

Very little work has been done in pure molten $MgCl_2$. Recent results [3] have shown that in this system diffusion control can also play a role in the cathodic discharge of Mg(II) species. This is probably due to diffusion of dissolved magnesium away from the electrode. Studies of the solubility of Mg in chloride melts have been reported. The solubility is low and increases as the activity of $MgCl_2$ increases [4]. It is proposed that dissolution of Mg leads to the formation of the subvalent species Mg_2^{2+} [5].

Structural studies of various halide melts, containing magnesium halides, by Raman spectroscopy have been reported by several authors [6, 7]. Raman spectroscopic studies of crystalline and molten $MgCl_2$ are reported by Capwell [8] and Huang and Brooker [9]. Capwell concluded, that the structure in pure molten $MgCl_2$ retains, to a large degree, the layer structure prevalent in the crystal. The existence of discreet complex molecular ions in the pure melt was not actually detected, but the presence of such species could not be excluded. According to Huang and Brooker [9], peaks which were assigned to $MgCl_4^{2-}$ tetrahedral complexes were found. They also found peaks which were probably due to symmetric stretching vibrations of polynuclear complexes. They suggested the following ion-pair formation:

$$Mg^{2+} + MgCl_4^{2-} = Mg_2Cl_4$$

Due to the relatively high conductivity of pure molten $MgCl_2$ Huang and Brooker [9] concluded that simple ions must also be present in pure molten $MgCl_2$.

2. Theory

Extremely high concentration of ions and high temperature are the two main reasons for the high exchange current densities of electrode reactions in molten salts. For these reasons the determination of their rates and mechanisms is impossible by the use of most classical electroanalytical methods. The existence of the high exchange current densities at the reversible electrodes immersed in their molten salts may be accounted for by using an equivalent circuit, which in addition to the double layer capacitance, also contains a double layer inductance [10, 11]. Contrary to the double layer capacitance, which describes the static properties of the electric double

0021-891X/93

layer at electrode interfaces, double layer inductance describes their dynamic properties.

It has been found in the previous studies [12–15] that simple charge transfer at a reversible electrode immersed in a pure molten salt can be described by the equivalent circuit presented in Fig. 1(a). If the electrode is immersed in a molten salt mixture, a diffusion process has to be taken into account (Fig. 1(b)). A two step electrode process in which the first step (low frequency) is quasireversible and the second (high frequency) is a pure charge transfer should be represented by the more complex equivalent circuit presented in Fig. 1(c).

The most useful method which can be used for the determination of the parameters of the equivalent circuits presented in Fig. 1 is electrochemical impedance spectroscopy (EIS). It has a very well developed theory for many different electrode processes [16, 17] together with computer programs for fitting of the experimental impedance spectra into a given equivalent circuit [18, 19]. As the charge transfer resistance of the electrode reactions at reversible electrodes in pure molten salts is very small (usually below 0.1Ω), the accuracy of the determination of the small charge transfer resistance is poor. Therefore, in the presented work here, a combination of the EIS and a RM with galvanostatic perturbation [10] is used.

If the reversible electrode represented by an equivalent circuit presented in Fig. 1(a) is perturbed by a short galvanostatic pulse, the resulting overpotential decay is described by the equation:

$$\eta(t) = \frac{\eta(0)}{s_2 - s_1}\left(s_1 \exp(-s_2 t) - s_2 \exp(-s_1 t)\right) \quad (1)$$

with

$$s_1 = \frac{R_{ct}}{2L_{dl}} + \left[\left(\frac{R_{ct}}{2L_{dl}}\right)^2 - \frac{1}{C_{dl}L_{dl}}\right]^{1/2} \quad (2)$$

$$s_2 = \frac{R_{ct}}{2L_{dl}} - \left[\left(\frac{R_{ct}}{2L_{dl}}\right)^2 - \frac{1}{C_{dl}L_{dl}}\right]^{1/2} \quad (3)$$

where $\eta(0)$ is the overpotential at zero time [10].

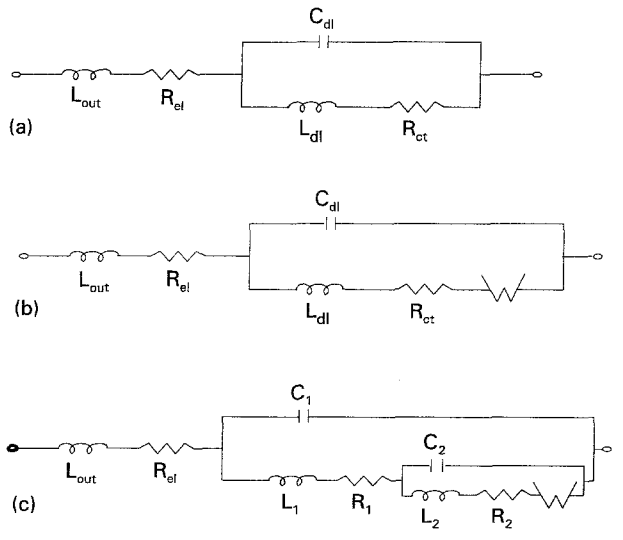

Fig. 1. Equivalent circuits.

It is seen in Equations 2 and 3 that the coefficients s_1 and s_2 represent certain angular frequencies. The computer fit of the experimentally recorded relaxation curve can be used to evaluate the frequencies s_1 and s_2 but these two quantities alone cannot provide all three parameters which describe the electric double layer in the equivalent circuit presented in Fig. 1(a). Either the double layer capacitance or the double layer inductance has to be provided by EIS. If the additional information from EIS is the double layer inductance, the charge transfer resistance is calculated by the equation:

$$R_{ct} = L_{dl}(s_1 + s_2) \quad (4)$$

If the electrode process is represented by the equivalent circuit in Fig. 1(b), the overpotential decay is described by the following equation [11]:

$$\eta(t) = A\exp(\alpha^2 t)\,\mathrm{erfc}(\alpha t^{1/2}) + B\exp(\beta^2 t)\,\mathrm{erfc}(\beta t^{1/2}) + C\exp(-\gamma t) \quad (5)$$

where A, B, C, α, β and γ are constants obtained from the experimental relaxation curve by the computer fitting procedure. The following important relationships hold:

$$\eta(0) = A + B + C \quad (6)$$

$$R_{ct} = L_{dl}(\alpha\beta + \gamma) \quad (7)$$

$$Z_W = L_{dl}(\alpha + \beta)\gamma \quad (8)$$

It is seen in Equations 7 and 8, that the low frequency charge transfer resistance and the Warburg diffusion impedance can be calculated from the constants α, β and γ, provided that the low frequency double layer inductance is obtained from separate impedance measurements.

3. Experimental details

3.1. *Materials*

Magnesium chloride-hexahydrate (p.a. Merck) was dried under HCl atmosphere up to 600 °C.

3.2. *Apparatus and procedure*

The experimental silica glass cell used for both relaxation and impedance measurements is presented in Fig. 2. The ceramic materials used inside the cell were heated up to 1200 °C in ambient atmosphere in a furnace to remove the adsorbed water. During the experiments the cell was purged with argon (grade 2) to prevent oxygen and moisture to enter the cell.

Pure metallic magnesium was used for all three electrodes, with the geometric area of the working electrode $A = 0.25 \pm 0.01\ \mathrm{cm}^2$.

The constant current pulse between the indicator and auxiliary electrodes was supplied by a PAR model 173 potentiostat–galvanostat with a PAR model 175 universal programmer. The relaxation of the

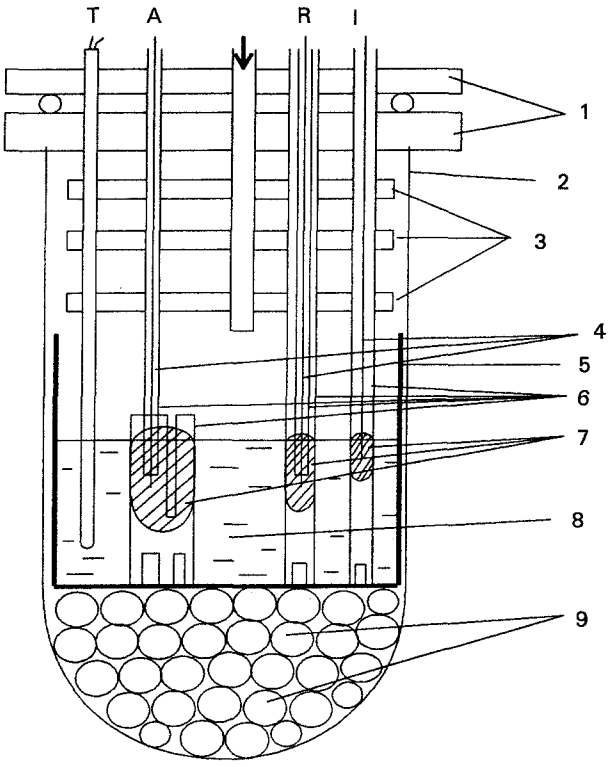

Fig. 2. The measuring cell: (1) brass lid, (2) quartz cell, (3) alumina shields, (4) Mo rod, (5) alumina crucible, (6) alumina tubes, (7) liquid Mg, (8) molten $MgCl_2$ and (9) ceramic rings.

overpotential of the working electrode (against the reference electrode) was recorded by a Nicolet 410 digitizing oscilloscope. The faradaic impedance spectra were recorded in the same cell using the computer controlled Solartron 1260 phase-gain analyser in two electrode configuration.

4. Results and discussion

4.1. *Equivalent circuit approach*

4.1.1. High frequency results. The impedance spectrum of the magnesium indicator electrode immersed in single molten magnesium chloride over a broad frequency range from 5 Hz to 1 MHz is presented in Fig. 3(a), whereas Fig. 3(b) presents the same spectrum as a Bode plot. As mentioned earlier, to obtain the high frequency charge transfer resistance for such an electrode reaction, the relaxation and the faradaic impedance method have to be combined. The computer fit of the faradaic impedance spectrum provides all parameters of the equivalent circuit presented in Fig. 1(c). In the frequency range from 100 Hz to 1 MHz there is no need to use any fixing procedure during the fit. The outer inductance is a constant, independent of the temperature, the value being a characteristic quantity for the given cell and the electrical furnace. For the set of results presented in the Table 1 the outer inductance was equal to $3.28 \pm 0.04\,\mu H\,cm^{-2}$. The electrolyte resistance decreased with increasing temperature, being around 10 Ω. The high frequency double layer inductance (L_1 in Fig. 1(c)) for the calculation of the high frequency charge transfer resistance by Equation 4 changes exponentially with

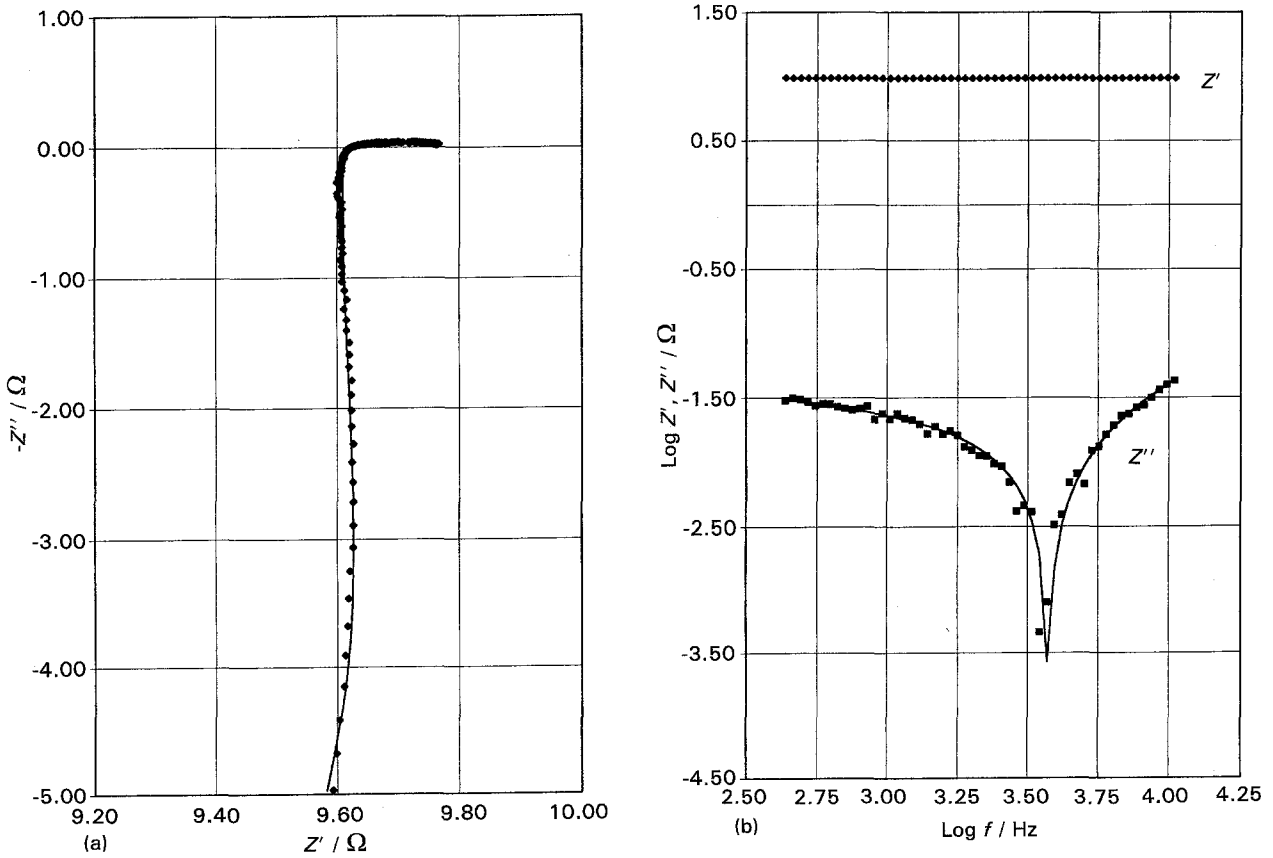

Fig. 3. Impedance spectrum of the magnesium electrode in molten $MgCl_2$ at 740 °C. (a) Complex impedance plot, (b) Bode plot. Markers: experimental values; lines: NLLS fit.

Table 1. Relaxation and impedance results for the high frequency step of the magnesium electrode reaction in molten $MgCl_2$

T / °C	$(s_1 + s_2)$ /10^3 s^{-1}	L_{dl} /μH
725	489	0.0336
740	497	0.0249
755	533	0.0269
770	512	0.0262
785	468	0.0226
800	470	0.0247
815	425	0.0223

the temperature [12–15]. Such behaviour is not surprising as, according to Equation 4, it has the feature of a kinetic quantity. The high frequency capacitance did not show any definite temperature dependence and, in the investigated temperature range, remained constant within experimental error at $30 \pm 5\,\mu F\,cm^{-2}$. In the frequency range from 5 Hz to 100 Hz the impedance of the auxiliary electrode had to be taken into account in the evaluation procedure.

The sum of the two frequencies $(s_1 + s_2)$ needed in Equation 4 was obtained by computer fit of the experimentally recorded relaxation curves. Typical overpotential decays (anodic and cathodic) are presented in Fig. 4.

Each relaxation curve, composed of 2000 points (time, overpotential) was fitted by a specially developed computer program, yielding, according to Equation 1, the two frequencies (s_1 and s_2). The double layer inductance, obtained from the computer fit of the impedance spectra, and the sum of the two frequencies (s_1 and s_2) obtained from the computer fit of the relaxation curves, are presented in the Table 1. The results are the mean values obtained at a given temperature by the computer fit of four separately recorded impedance spectra and eight relaxation curves.

Table 2 presents the summary of the kinetic data of the high frequency step. The charge transfer resistance, calculated from the data presented in Table 1, was used for the calculation of the exchange current density j_0 by the equation:

$$j_0 = \frac{RT}{FR_{ct}} \tag{9}$$

4.1.2. Low frequency results. The parameters of the low frequency loop of the equivalent circuit presented in Fig. 1(b) were obtained from the computer fit in the frequency range from 400 to 10 000 Hz. The high frequency impedance spectrum, according to the equivalent circuit presented in Fig. 1(a), was subtracted from the total spectrum and the possible influence of the counter electrode impedance was also taken into account. The main parameters obtained from this fit are the low frequency charge transfer resistance and the low frequency double layer inductance. These values at several temperatures are presented in Table 3. The Warburg diffusion impedance obtained from the fit is not very accurate but decreases slightly with increasing temperature. To calculate more accurate values of the low frequency charge transfer resistance and the Warburg diffusion impedance by the use of Equations 7 and 8, the constants α, β and γ must be determined from the relaxation curves in the millisecond range.

It is seen in Fig. 4, that the transients in the microsecond range do not drop to zero, since the diffusional part relaxes in the ms range. Typical recordings of the

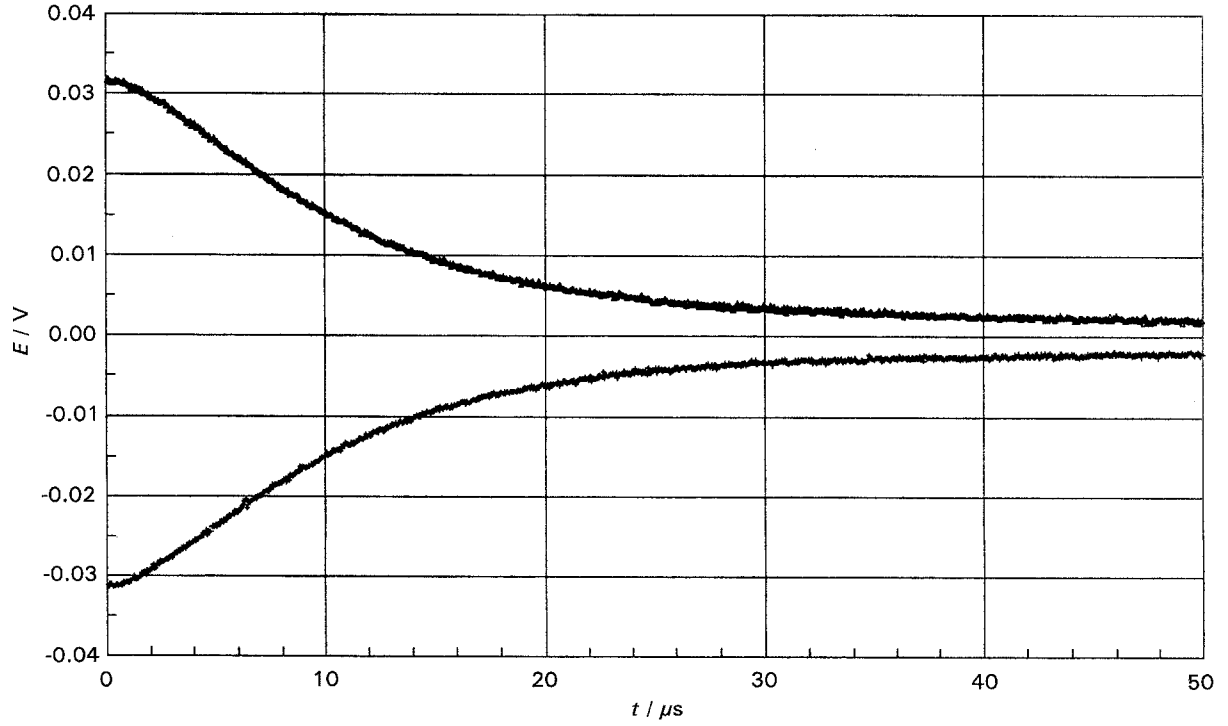

Fig. 4. Anodic and cathodic microsecond relaxation curves after galvanostatic perturbation of the magnesium working electrode in molten $MgCl_2$ at 800 °C. Current density of perturbation: 2.2 A cm^{-2}. Time of perturbation 0.1 ms.

Table 2. Kinetic parameters of the high frequency step of the magnesium electrode reaction in molten $MgCl_2$

T / °C	R_{ct} /Ω cm^2	j_0 /A cm^{-2}
725	0.004 16	20.6
740	0.003 08	28.3
755	0.003 58	24.7
770	0.003 36	26.7
785	0.002 66	34.2
800	0.002 91	31.7
815	0.002 37	39.4

Table 3. Low frequency inductance and charge transfer resistance of the magnesium electrode reaction in molten $MgCl_2$ as obtained from the fitting of the impedance spectra

T / °C	L_{dl} /μH cm^2	R_{ct} /Ω cm^2
725	0.945	0.0520
740	0.827	0.0450
755	0.705	0.0417
770	0.740	0.0400
785	0.715	0.0357
800	0.672	0.0390
815	0.622	0.0332

millisecond relaxation times after cathodic and anodic perturbation of the magnesium electrode in pure molten $MgCl_2$ are presented in Fig. 5.

As seen in Fig. 5 the perturbation is fairly small (a few millivolts). In contrast to Fig. 4, the overpotential now drops to zero, as with this decay the whole electrode process has returned to equilibrium.

Such relaxation curves at several temperatures were fitted into Equation 5 to get the values of the constants α, β and γ. Although small differences between cathodic and anodic relaxation curves were seen, the results of fitting at several temperatures, presented in Table 4 are the mean values of both types of relaxation curve.

Table 4. Constants α, β and γ of Equation 5 obtained from the fit of millisecond relaxation curves at several temperatures

T / °C	α /s$^{-1/2}$	β /s$^{-1/2}$	γ /s^{-1}
725	239	149	6572
740	259	150	6522
755	244	151	5585
770	291	149	5625
785	245	150	5440
800	228	151	5153
815	171	150	4284

Table 5. Low frequency kinetic data and Warburg diffusion impedance of the magnesium electrode in molten $MgCl_2$ at several temperatures

T / °C	R_{ct} /Ω cm^2	j_0 /A cm^{-2}	Z_w /Ω s$^{-1/2}$
725	0.0400	2.15	2.41
740	0.0372	2.34	2.17
755	0.0322	2.75	1.55
770	0.0365	2.46	1.83
785	0.0300	3.04	1.53
800	0.0265	3.48	1.30
815	0.0228	4.11	0.83

Using the constants α, β and γ from Table 4 and the low frequency double layer inductance from Table 3 it is possible to calculate more accurate values of the low frequency charge transfer resistance and the Warburg diffusion impedance by Equations 7 and 8. The results of calculations are presented in Table 5.

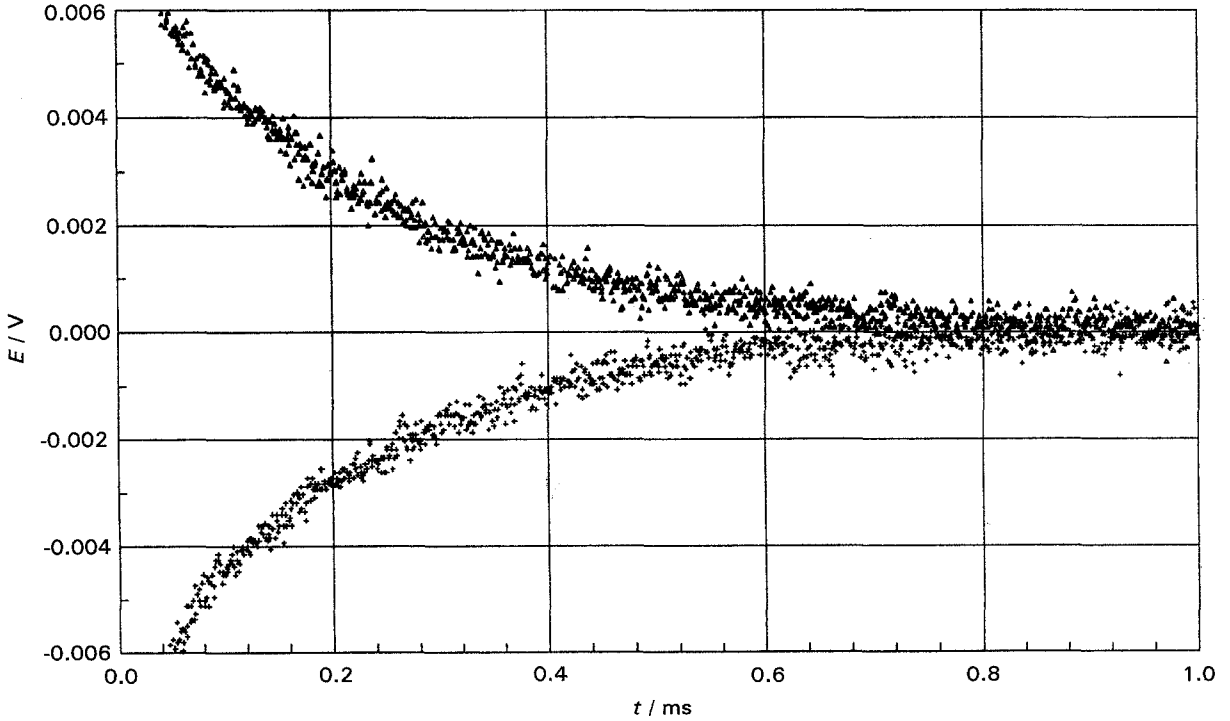

Fig. 5. Anodic and cathodic millisecond relaxation curves after galvanostatic perturbation of the magnesium working electrode in molten $MgCl_2$ at 800 °C. Current density of perturbation: 3.4 A cm^{-2}. Time of perturbation 0.1 ms.

Table 6. Parameter values for the Mg electrode when including a preceding chemical step

T /°C	R_{ct} /Ω cm^2	σ_O /Ω s$^{-1/2}$	σ_R /Ω s$^{-1/2}$	σ /Ω s$^{-1/2}$	K	k /s^{-1}
725	0.0556	1.26	2.91	4.17	0.22	9000
740	0.0501	0.99	2.21	3.20	0.30	7500
755	0.0471	1.09	2.40	3.49	0.26	6500
770	0.0352	0.58	2.19	2.77	0.30	6000
785	0.0322	0.87	1.80	2.67	0.27	5900
800	0.0352	0.70	1.56	2.26	0.33	5600
815	0.0290	0.62	1.40	2.02	0.40	5000

4.2. *Chemical approach*

If a polynuclear complex like Mg_2Cl_4 (or $(MgCl_2)_n$) exists in pure molten $MgCl_2$, then a slow dissociation of this complex would reflect the kinetics of the electrode reaction. Such a dissociation process may be handled as a preceding chemical reaction, followed by two charge transfer steps:

$$(MgCl_2)_n \underset{k_2}{\overset{k_1}{\Longleftrightarrow}} Mg^{2+} + Mg_{n-1}Cl_{2n}^{2-} \quad (10)$$

$$Mg^{2+} + e^- \Longleftrightarrow Mg^+_{(ads)} \quad (11)$$

$$Mg^+_{(ads)} + e^- \Longleftrightarrow Mg \quad (12)$$

Step 11 represents the low frequency charge transfer and Step 12 the high frequency charge transfer, not influenced by diffusion.

With the assumption of the above mechanism, it should be possible to fit the low frequency impedance spectra, by the following reaction impedance equations derived for the CE mechanism by several authors [20–22]:

$$Z_r = Z'_r - iZ''_r \quad (13)$$

with

$$Z'_r = R_{ct} + \sigma_R\omega^{-1/2} + \frac{K}{1+K}\sigma_O\omega^{-1/2} + \frac{1}{1+K}\sigma_O\left[\frac{(\omega^2+k^2)^{1/2}+k}{\omega^2+k^2}\right]^{1/2} \quad (14)$$

$$Z''_r = \sigma_R\omega^{-1/2} + \frac{K}{1+K}\sigma_O\omega^{-1/2} + \frac{1}{1+K}\sigma_O\left[\frac{(\omega^2+k^2)^{1/2}-k}{\omega^2+k^2}\right]^{1/2} \quad (15)$$

In the above expressions

$$\sigma = \sigma_O + \sigma_R = \frac{RT}{n^2F^2A\sqrt{2}}\left(\frac{1}{D_R^{1/2}C_R^*} + \frac{1}{D_0^{1/2}C_0^*}\right) \quad (16)$$

is related to the Warburg impedance, and

$$k = k_1 + k_2 \quad (17)$$

is related to the rates of the preceding chemical

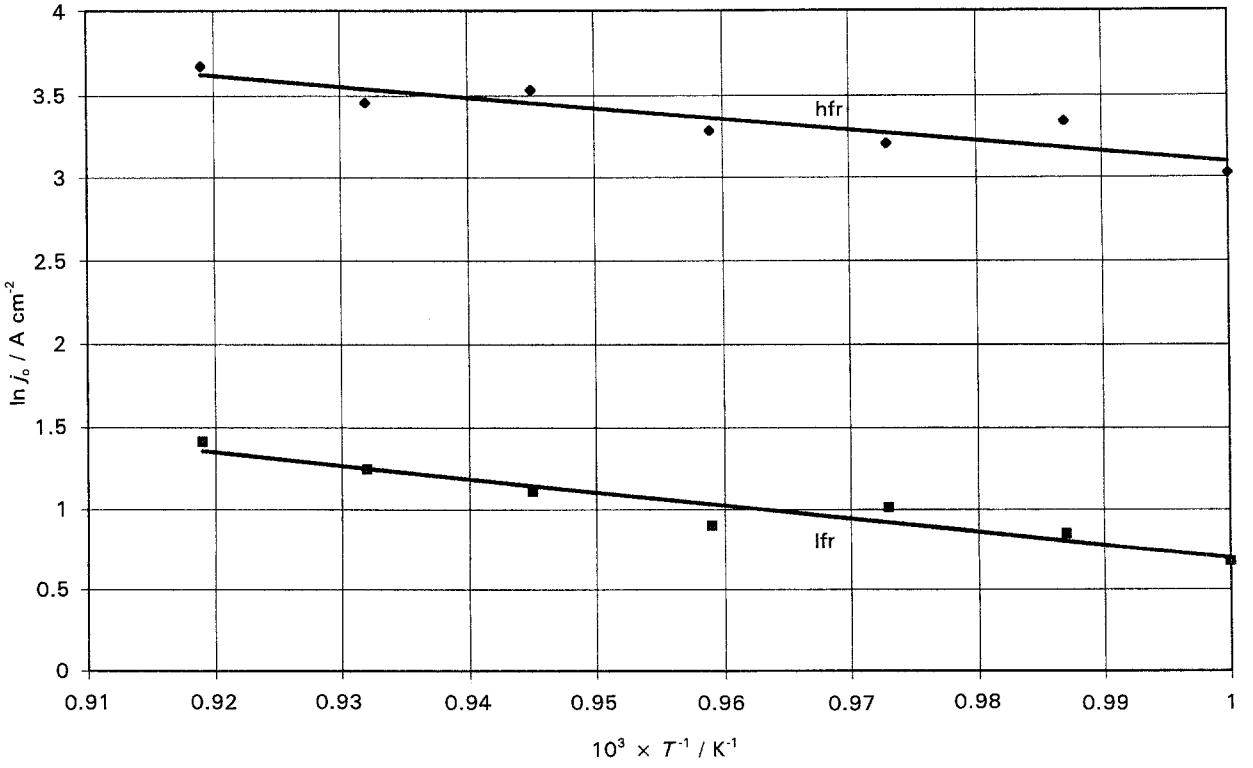

Fig. 6. Arrhenius plots of the exchange current densities of the magnesium electrode reaction in pure molten $MgCl_2$.

reaction, and

$$K = k_1/k_2 \tag{18}$$

is the equilibrium constant of the preceding chemical reaction.

To work out the low frequency impedance spectra in terms of a preceding chemical reaction, that part of the impedance spectra corresponding to the high frequency step (including outer inductance and the electrolyte resistance) was first subtracted by the use of the DATA CRUNCHER in the EQUICIRCUIT program [18]. The remaining impedance spectrum was fitted by a special program based on the above equations in the low frequency range. The results, at several temperatures are presented in Table 6.

The values of the charge transfer resistance for the low frequency step are listed three times, obtained directly from the impedance fit in Table 3, from the combination of the impedance and relaxation results in Table 5 and with consideration of the preceding chemical step in Table 6. The discrepancy is moderate with the directly obtained values in Table 3 about 20% lower than the values from the two other procedures. The corresponding low frequency value of the exchange current density, which corresponds to the first step of the cathodic discharge reaction in pure molten $MgCl_2$, is in fair agreement with the value quoted in the literature [2, 3].

The temperature dependence of the exchange current densities of the high and low frequency steps of the magnesium electrode reaction are presented in the form of Arrhenius plots in Fig. 6.

The straight lines representing the Arrhenius plots in Fig. 6 are

$$\ln j_{0,hf} = 9.5433 - \frac{6444}{T} \tag{19}$$

and

$$\ln j_{0,lf} = 8.0441 - \frac{7296}{T} \tag{20}$$

giving rise to the activation energies of 53.5 and $60.6\,\mathrm{kJ\,mol^{-1}}$ for the high frequency and low frequency steps, respectively.

5. Conclusions

It follows from the results, that the mechanism of the magnesium electrode reaction is a three step process. The first one, which above has been referred to as the low frequency step, is preceded by a dissociation reaction and connected with diffusion of the Mg(II) ions in the melt. Diffusion is not pronounced as the diffusion impedance, of the order of $1.5\,\Omega\,s^{-1/2}$, is actually very small.

The dissociation reaction (Equation 10) does not correspond exactly to the assumed first order preceding reaction in the derivation of Equations 14 and 15. In spite of this, the exchange current densities are very much the same as those obtained by the equivalent circuit approach above. The mechanism of the electrode reaction on a liquid magnesium electrode immersed in pure molten $MgCl_2$, and represented by Equations 10–12, has thus been confirmed. In our opinion the combination of the relaxation and faradaic impedance method, presented in the equivalent circuit approach, gives the most accurate values of both the charge transfer resistance and the Warburg diffusion impedance.

References

[1] G. M. Rao, *J. Electroanal. Chem. Interfacial Electroch.* **249** (1988) 191.
[2] R. Tunold, 'Light Metals', *Trans. Metall. Soc.*, AIME, (1980) p. 949.
[3] B. Børresen, G. Haarberg, R. Tunold and O. Wallevik. Proceedings of the international symposium on molten salt chemistry and technology, Honolulu, HI, The Electrochemical Society, NY, USA **93-9** (1993) p. 193.
[4] J. Wypartowicz, T. Ostvold and H. A. Øye, *Electrochim. Acta* **25** (1980) 151.
[5] J. D. van Norman and J. J. Egan, *J. Phys. Chem.* **67** (1963) 2460.
[6] M. H. Brooker and C. H. Huang, *Can. J. Chem.* **58** (1980) 168.
[7] V. A. Maroni, E. J. Hathaway and E. J. Cairns, *J. Phys. Chem.* **75** (1971) 155.
[8] R. J. Capwell, *Chem. Phys. Lett.* **12** (1972) 443.
[9] C. H. Huang and M. H. Brooker, *ibid.* **43** (1976) 180.
[10] A. Kisza, *Polish J. Chem.* **67** (1993) 885.
[11] *Idem, ibid.* **68** (1994) 613.
[12] A. Kisza and J. Kaźmierczak, *ibid.* **68** (1994) 329.
[13] J. Thonstad and A. Kisza, 'Molten salt forum' Vols. **1–2**, Trans. Tech. Publications, Aldermannsdorf, Switzerland (1993–94) p. 195.
[14] J. Thonstad, A. Kisza and J. Kaźmierczak, *J. Appl. Electrochem*, in press.
[15] A. Kisza, J. Kaźmierczak, B. Børresen, G. M. Haarberg and R. Tunold, *J. Electrochem. Soc.*, **142** (1995) 1035.
[16] A. J. Bard, R. L. Faulkner, 'Electrochemical methods, fundamentals and applications', John Wiley, New York (1980).
[17] J. Ross Macdonald, 'Impedance spectroscopy', John Wiley, New York (1987).
[18] B. Boucamp, 'Equivalent circuit', University of Twente, Holland (1988–89).
[19] J. Ross Macdonald, Complex nonlinear least squares immittance fitting program', Department of Physics and Astronomy, University of North Carolina, Chapel Hill, NC.
[20] D. E. Smith, 'Electroanalytical chemistry', vol. 1, (edited by A. J. Bard), Dekker, New York (1966) p. 1.
[21] M. Sluyters-Rehbach and J. H. Sluyters, 'Electroanalytical chemistry', vol. 4, (edited by A. J. Bard), Dekker, New York (1970) p. 1.
[22] H. Matsuda, P. Delahay and M. Kleinermann, *J. Am. Chem. Soc.* **81** (1979) 6379.